Polymer Diffusion in Linear Matrices: Polystyrene in Toluene

Hongdoo Kim, Taihyun Chang,† James M. Yohanan,‡ Lixiao Wang, and Hyuk Yu*

Department of Chemistry, University of Wisconsin, Madison, Wisconsin 53706.
Received April 18, 1986

ABSTRACT: The translational diffusion coefficient of polystyrene, labeled with azobenzene derivatives and having a molecular weight range $10^4 \leq M \leq 1.8 \times 10^6$, has been studied in matrices of the same polymer in toluene with the technique of forced Rayleigh scattering. The independent variables were the matrix concentration C and molecular weight M of the labeled (tracer) polymer, over a wide range of the matrix molecular weight $10^4 \leq M_p \leq 8.4 \times 10^6$. The diffusion coefficient of the tracer polymer D_{tr} at 20 °C is found to be sensitive to M_p until $M_p \geq (3\text{–}5)M$; when M_p exceeds this limit, D_{tr} no longer depends on M_p and we call D_{tr} at such a limit the asymptotic tracer diffusion coefficient D_{tr}^{∞}. *In the context of the reptation model*, the M_p dependence of D_{tr} is interpreted as evidence for a substantial extent of the tube renewal process in semidilute solutions. At the high ends of M ($\sim$(1–2) $\times 10^6$) and C ($\sim$10–20 wt %), $D_{tr}^{\infty} \propto M^{-3}C^{-3}$ is a better representation of the data than $D_{tr}^{\infty} \propto M^{-2}C^{-1.75}$. Further, D_{tr}^{∞} is shown to scale with (C/C^*) in semidilute solutions for $3.5 \times 10^4 \leq M \leq 1.8 \times 10^6$.

Introduction

The dynamics of polymer chains above the overlap concentration has been extensively studied recently in conjunction with the development of scaling ideas[1] and the reptation model.[2–4] Among various dynamic properties, the self-diffusion coefficient is the one receiving the most attention in the literature. Its popularity comes not only from the recognition of its fundamental importance, associated with the terminal relaxation process of polymer chains, but also from the availability of a host of different experimental techniques in recent years.[5–14] A substantial body of experimental data as well as new experimental techniques has been reviewed recently.[15] It is still true, however, that our knowledge of polymer chain dynamics is far from complete, and the apparent initial success of the reptation model seems to have been somewhat clouded as more experimental data have been accumulated. In order to address the problem clearly, we will first summarize the current status of our understanding of polymer self-diffusion in two parts, polymer melts (bulk state) and semidilute solutions.

In polymer melts, there seems to be good agreement between experiment and theoretical prediction in terms of the molecular weight dependence of self-diffusion coefficients, $D \propto M^{-2}$. The major discrepancies found in some experiments have been taken care of by considering some additional effects beyond the simple reptation picture. For instance, the M^{-2} dependence observed far below the entanglement molecular weights, where such a behavior is not expected, has been explained by taking into account the chain end free volume contribution to the local friction.[16] Also, the tube renewal or constraint release process has been examined experimentally,[13] and the results appear to be consistent with the theoretical prediction.[17,18] Experiments with nonlinear polymers such as stars[19] showed remarkable differences from linear polymers which are again qualitatively consistent with the reptation model, whereas with rings[20,21] the results are not very different, which is inconsistent with the model. Perhaps the central question is whether the consistency constitutes a confirmation of the reptation model. Certainly the observed M^{-2} dependency is not a sufficient condition, possibly only a necessary one, to validate the model. In particular, the higher power molecular weight dependence of observed viscosity over that of the theoretical prediction has been the major blemish of the reptation model and some modifications or alternative models have been proposed.[22–29] Nevertheless there is a consensus that the majority of currently available self-diffusion data is successfully explained by the reptation theory.

Turning to the case of semidilute solutions, the agreement between theory and experiment is far less spectacular. Since Leger et al.[9] reported $D \propto M^{-2}C^{-1.75}$ in good solvents, which is exactly the prediction of the reptation with scaling theory, most subsequent experiments have shown the −1.75 exponent over a quite limited concentration range only.[10,30,31] Recently, a concentration-dependent local viscosity correction in terms of the friction felt by small tracer molecules has been proposed,[32] and it has been somewhat successful in expanding the concentration range where the appropriate exponent of concentration dependence is observed. The proposal, however, ought to be regarded as at best a first-order approximation since hydrodynamic interactions are ignored whereas they should play an important role inside a hydrodynamic correlation length, particularly in the low-concentration regime below $\sim$10%.

The predicted concentration and molecular weight power exponents of polymer self-diffusion in solutions above the overlap concentration C^* are the consequences of two separate concepts, hydrodynamic screening and reptation. To put it another way, the interpenetrating polymer chains effectively segregate a whole chain into hydrodynamically screened concentration blobs that behave like Rouse segments, and the whole Rouse chain, composed of these blobs strung together, reptates through a tube delineated by the surrounding chains. Of these two concepts, the hydrodynamic screening has been well examined by mutual diffusion[33] and sedimentation measurements.[34] Given that there exists a well-defined hydrodynamic screening length and its power law dependence on concentration is firmly established, poor agreement of the observed concentration dependence of the self-diffusion coefficient with the theory remains a serious pending problem for the reptation model.

In this work, we examine the problem further by following the diffusion coefficients of tracer polymer molecules dispersed in a matrix composed of the same polymer with differing chain lengths. Both the tracer and matrix polymer are of wide ranges of molecular weights in the semidilute solution regime. With this set of experiments we attempt to scrutinize the polymer diffusion in a truly semidilute regime where the local friction contribution is

† Present address: Korea Research Institute of Chemical Technology, Daeduck Danji, Daejeon 300-32, Republic of Korea.
‡ Present address: School of Medicine, University of Wisconsin—Madison, Madison, WI 53706.

0024-9297/86/2219-2737$01.50/0

Table I
Summary of Sample Characteristics

sample	$M_w \times 10^{-3}$	M_w/M_n	source and lot no.
10k	10	<1.06	PC 8b
35k	35	1.06	PC 80317
51k	51	<1.06	PC 7a
100k	100	1.06	PC 70111
390k	390[a]	1.06	PC 00507
900k	929	1.10	PC 80323
1800k	1760	1.15	PC 30622
3800k	3840	1.04	TS 34
8400k	8420	1.17	TS 31

[a] Molecular weight provided by the manufacturer is quoted as 293 000. It is separately determined to be 390 000 by light scattering and GPC by Dr. Elizabeth V. Patton of Kodak Research Laboratories. PC and TS stand for Pressure Chemicals and Toyo Soda, respectively.

negligible while keeping the constraint release process to a minimum. This can be done by using matrices of much higher molecular weights than the tracer polymers so that the matrix molecular weight dependence of the tracer diffusion coefficients vanishes. The matrix effect was examined earlier by Leger et al.,[9] though not extensively, and they concluded that the tube renewal process is weak at the self-diffusion limit. Pursuing this point, we believe a more systematic study is certainly called for, particularly since it has been shown that the tube renewal process may contribute rather significantly to the self-diffusion of low molecular weight polymer chains in melts.[13] In terms of the number of equivalent Rouse segments, a given polymer chain in a semidilute solution has a smaller number of entangled units than in the bulk state, so that the tube renewal process should contribute much more in solutions. Also, by varying the size of the tracer diffusant gradually over a wide range from a small tracer molecule through the size of the concentration blobs of the matrix, we can gain access to the issue of local friction whereby the validity of the proposal for local viscosity correction can be evaluated. This will eventually lead us to assess the role of hydrodynamic screening in the tracer diffusion. Having thus examined the extent of contributions by tube renewal and hydrodynamic screening, we then focus on the reptation process as to whether it indeed governs the transport mechanism in semidilute solutions.

Among the different techniques that have been applied to measure the tracer diffusion of polymer chains, forced Rayleigh scattering[9-11] (FRS) is a natural choice since it allows the most freedom in varying diffusants and matrices. Although the technique suffers from violation of sample integrity owing to its requirement of sample modification, the labeling is what makes the technique unique in this circumstance. Furthermore, we recently found a much better procedure for labeling polymer chains randomly than was used in our previous work[10] so that our signal-to-noise ratio has been greatly improved while the chemical perturbation is kept to a minimum.

Experimental Section

1. **Labeling of Polystyrene.** Polystyrenes used in this study are commercial samples (Pressure Chemical Co. and Toyo Soda Co.) and their characteristics are summarized in Table I. The labeling procedure starts with a random aminomethylation of phenyl rings in polystyrene by the procedure of Mitchell et al.[35] with some modifications. The aminomethyl groups were subsequently reacted with an appropriate azo dye to complete the labeling procedure. Detailed procedures are as follows.

(a) Aminomethylation of Polystyrene. One gram of polystyrene and a calculated amount of *N*-(hydroxymethyl)phthalimide (I) are dissolved in 300 mL of CH_2Cl_2, and then 100 mL of trifluoroacetic acid is added to the solution. For this work the

Scheme I

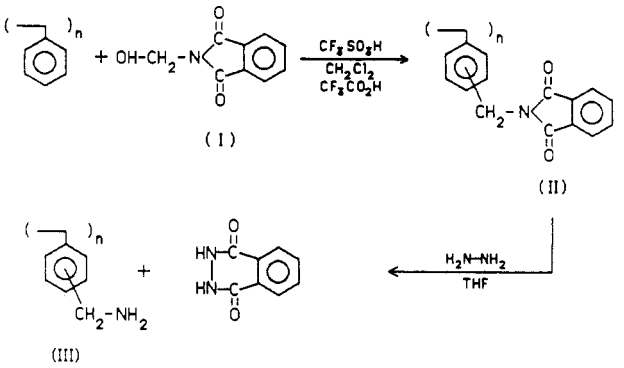

molar ratio of monomer units of polystyrene and *N*-(hydroxymethyl)phthalimide is 300:1. If the solution becomes turbid, more CH_2Cl_2 is added until turbidity disappears. Trifluoromethanesulfonic acid (0.5 mL) as a catalyst is then added, and the solution is stirred for 4 h at room temperature. At the end of the reaction, the intermediate II is precipitated in methanol and washed once more by dissolving in tetrahydrofuran and reprecipitating in methanol. The characteristic carbonyl stretching bands of the infrared spectrum at 1720 and 1775 cm^{-1} are observed to confirm the formation of methylphthalimide groups. Also, a GPC chromatogram (Waters Associates, Milford, MA) is taken to ascertain that the molecular weight distribution has not been altered by this reaction. Either excess catalyst or longer reaction time is found to induce cross-linking of polymers, but it can be controlled without difficulty. The intermediate II is then dissolved in 100 mL of tetrahydrofuran containing 2 mL of hydrazine and refluxed for 2 days. After the reflux, the aminomethylated polystyrene III is purified by precipitating it in methanol. The cleavage of the phthalimide group and the formation of the aminomethyl group are confirmed to proceed quantitatively by infrared spectroscopy. At this point, a GPC chromatogram of aminomethylated polystyrene shows a slightly longer tail than that of the starting polymer, which we attribute to the interaction of amino groups of eluted polymer and the column packing of polystyrene beads. The chemistry of the labeling is schematically shown in Scheme I.

(b) Dye Labeling. Three different azo dyes, namely, (dimethylamino)azobenzene isothiocyanate (IV) (Pierce, Rockford, IL), phenylazobenzoyl chloride (V) (Kodak), and [(dimethylamino)phenyl]azobenzoic acid (VI) (Kodak), are used for this work.

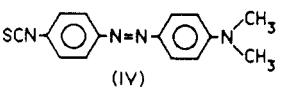

(IV)

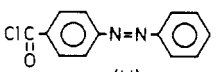

(V)

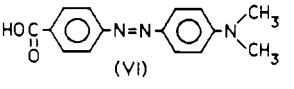

(VI)

These dyes have slightly different characteristics. For instance, IV and VI show much better contrast, generating a strong FRS signal, but have a shorter photochromically shifted state lifetime than V. However, the diffusion coefficient of labeled polymers is found to be independent of the labels and the best dye for the specific use was appropriately chosen with the two factors in mind. Final dye labeling is carried out by dissolving aminomethylated polystyrene III in THF containing an excess of a chosen dye and stirring at room temperature for a few days. When VI is used, dicyclohexylcarbodiimide is added as a coupling reagent.[36,37] The dye content of labeled polystyrene is determined spectrophotometrically, and it was found that the labeling ratio is practically the same as the stoichiometric ratio of monomer unit of polystyrene and *N*-(hydroxymethyl)phthalimide used. Therefore, under the reaction conditions illustrated in Scheme I, all the

reaction steps seem to go quantitatively. The final product at the conclusion of the labeling procedure was also examined by GPC, and it was confirmed to have a chromatogram indistinguishable from that of the starting polymer.

2. Forced Rayleigh Scattering Measurements. Samples for FRS measurements were prepared by adding a small amount of labeled polystyrene, typically 0.05 wt % of the whole sample, to an appropriate amount of matrix polystyrene in toluene and allowing the polystyrenes to mix completely with occasional shaking. After the complete dissolution of polystyrene, which takes up to a few days for high molecular weight samples, the solution was directly filtered through a 0.45-μm-pore poly(tetrafluoroethylene) membrane filter (Bio-Rad, Richmond, CA) into a precleaned 5-mm path length spectrophotometer cuvette for FRS measurements. For either high-molecular-weight or high-concentration samples where direct filtrations were difficult, more dilute samples were prepared and filtered, and the excess solvent was slowly evaporated under dust-free conditions to obtain the desired concentrations in an optically clear state. The optical configuration of the FRS instrument, similar to that of Leger et al.,[9] and the data acquisition and analysis scheme are the same as in our previous work[38] from this laboratory, and all the experiments were performed at 20.0 ± 0.1 °C.

Most of the decay profiles can be fit with a single-exponential model function by using the typical relation[9]

$$V(t) = (Ae^{-t/\tau} + B)^2 + C^2 \quad (1)$$

In certain cases, however, the decay profiles deviate markedly from single exponential. When such a non-single-exponential decay was observed, a second-order cumulant model function

$$V(t) = [A' \exp(-t/\tau + B't^2)]^2 + C'^2 \quad (2)$$

was used to fit the data. In these cases, the parameter B in eq 1, which represents the coherent background optical field, is neglected because it is strongly coupled with the second cumulant B' and sometimes leads to anomalous results. The omission of the parameter B usually does not make a significant difference in the final results for either model function since a typical signal-to-background ratio is about 100; we attribute this to our efforts to clean the samples and cells scrupulously. In any case, the final criterion to accept a given set of measurements is the reproducibility of the decay profiles and the confirmation of the decay time constant (τ) dependence on the scattering wave vector q, $\tau^{-1} \propto q^2$. Having determined the results over more than five different angles, we obtained the diffusion coefficient from the slope of a least-squares fit according to the relation[39]

$$1/\tau = 1/\tau_{life} + Dq^2 \quad (3)$$

Here, τ is the measured decay time constant, τ_{life} is the lifetime of the photochromically shifted state of the dye, and D is the diffusion coefficient.

Results and Discussion

Comparison of Self-Diffusion Coefficient with Mutual Diffusion Coefficient. In Figure 1 are displayed the diffusion coefficients of labeled 900k polystyrene by FRS and those of the unlabeled, but otherwise the same, sample by quasi-elastic light scattering (QELS). The mutual diffusion coefficients, measured by QELS, increase with polymer concentration as scaling theory predicts, and a straight line is drawn to show the concentration power law exponent 0.67 in good solvents, which was first observed by Adam and Delsanti[33] and subsequently by many others.[40,41] On the other hand, the tracer diffusion coefficients measured by FRS drop rapidly with concentration so that the two diffusion coefficients at a concentration of 10 wt % are almost 3 orders of magnitude apart. Although the whole profile of the concentration dependence of the tracer diffusion coefficients would be best represented by a smooth curve, two straight lines are drawn according to the scaling law predictions in order to compare the limiting slopes. We will come back to the discussion of the power law exponents later. For now, we focus on

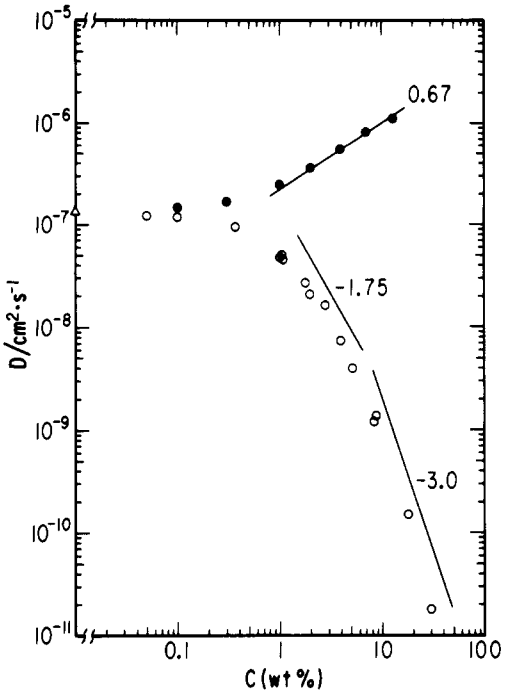

Figure 1. Mutual diffusion and self-diffusion coefficients as functions of the concentration of 900k polystyrene in toluene at 20 °C. Filled circles denote the mutual diffusion coefficients of the polystyrene (without photolabels) by quasi-elastic light scattering and open circles denote the self-diffusion coefficients of the labeled polystyrene by forced Rayleigh scattering. The infinite dilution diffusion coefficient D_0 reported by Appelt and Meyerhoff[42] is indicated on the ordinate, and both mutual and self-diffusion coefficients are seen to merge to the same D_0 value. A 0.67 slope is drawn through the mutual diffusion coefficients in accordance with Adam and Delsanti.[33] Although the self-diffusion coefficients appear to be represented by a smooth curve over the entire concentration range, −1.75 and −3.0 slopes are drawn to show apparent power law ranges.

how both the mutual and tracer diffusion coefficients merge to the same value at the infinite dilution limit, as should be. Although this may appear to be a trivial achievement, few techniques for tracer diffusion have been thus calibrated against other established techniques. Much more important is the fact that our labeling method confers sufficient sensitivity to FRS signals so that we can extrapolate the measured diffusion coefficient to the infinite dilution limit without ambiguity. Further, the perturbation of the sample is small enough to ensure the coincidence of the mutual diffusion coefficient (without labeling) and the tracer diffusion coefficients (with labeling) at infinite dilution.

Matrix Molecular Weight Dependence of Tracer Diffusion. The q^2 dependence of the decay time constants of the FRS signal is displayed in Figure 2. This particular set of data is obtained from the sample containing 0.05 wt % 900k labeled polystyrene in 2.0 wt % of unlabeled polystyrene of various molecular weights as the matrices. As molecular weight of the matrix increases, the plot shows a gradual decrease of the diffusion coefficient of tracer polystyrene, which is represented as the slope of the plot according to eq 3. Contrary to the generally accepted notion, the tracer diffusion coefficient of 900k polystyrene does not reach the asymptotic value at the matrix molecular weight of 900k, which is the self-diffusion limit of the polymer. Instead, a much higher molecular weight is required to make the matrix molecular weight dependence disappear, as exhibited by the almost indistinguishable slopes at the matrix molecular weights of 3.8×10^6 and 8.4×10^6. When we plot the tracer dif-

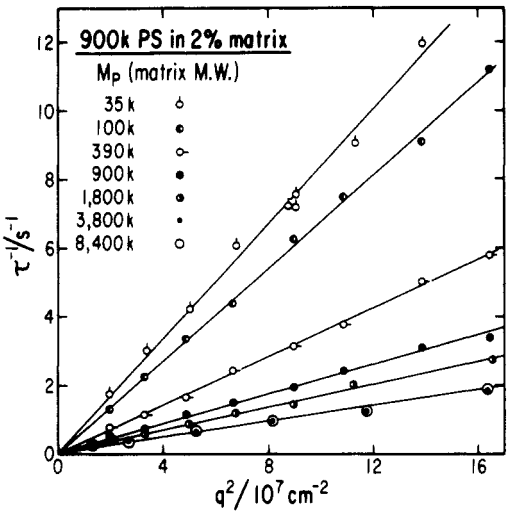

Figure 2. Plot of inverse decay time constant τ^{-1} of 900k labeled polystyrene against the square of the scattering vector q^2 in 2 wt % of matrix polystyrene of different molecular weights at 20 °C. The molecular weights of matrix polystyrene are identified by different symbols. The tracer diffusion coefficient is obtained according to eq 3; each slope corresponds to the tracer diffusion coefficient of 900k polystyrene at a given matrix molecular weight.

fusion coefficient as a function of matrix molecular weight as in Figure 3, we must note two distinctive features. First, the tracer diffusion coefficient settles down only after the matrix molecular weight reaches at least a factor of 3–5 higher than that of tracer polymers. Second, the onset matrix molecular weight (M_p^*) exhibiting the asymptotic diffusion coefficient (D_{tr}^∞) does not seem to change much with matrix concentration. This should be contrasted to the entanglement coupling molecular weight in a given concentration $M_c(C)$ which is inversely proportional to concentration C, $M_c(C) = \rho M_c/C$, where ρ and M_c are the polymer bulk density and entanglement coupling molecular weight at bulk state, i.e., 35k for polystyrene, respectively.

We now turn to the significance of these two points. *In the context of the reptation model*, the first observation can be taken to confirm that the tube renewal process contributes significantly to tracer diffusion in semidilute solutions unless the matrix molecular weight is substantially higher than that of the diffusant. In other words, the tube renewal process is by no means a weak process at the self-diffusion limit. Hence, the self-diffusion measurements in semidilute solutions hitherto reported in the literature cannot be accepted as lending support to the reptation model by themselves without explicitly taking into account the tube renewal process. Alternatively, we could interpret the results without resorting to the reptation model; the dynamic processes, of whatever origins, of the matrix contribute substantially to the self-diffusion. The second observation of relative invariance of M_p^* with respect to matrix concentration makes our results difficult to reconcile with the reptation model. One of its consequences is that the tube renewal process will progressively be weakened as the matrix concentration is raised. This is because the number of entangled subunits or hydrodynamically isolated Rouse segments increases in a polymer chain as the concentration of the matrix increases, and the theory predicts the contribution of the tube renewal process to diminish rapidly as the number of subunits increases.[17,18] Our observation does not follow such a predicted behavior.

Concentration Dependence of D_{tr}^∞. We now focus on the asymptotic tracer diffusion coefficient, designated

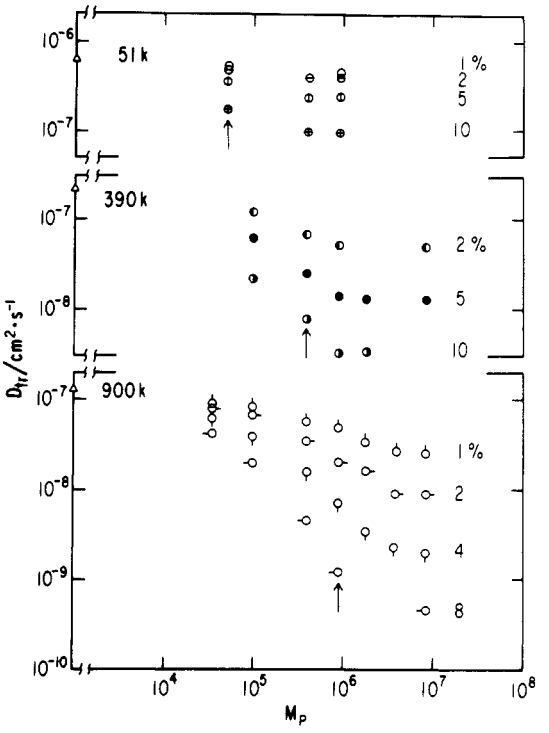

Figure 3. Matrix molecular weight (M_p) dependence of the tracer diffusion coefficient D_{tr} at 20 °C. The tracer polymers, 51k, 390k, and 900k, are denoted in all three graphs, and their diffusion coefficients at infinite dilution as reported by Appelt and Meyerhoff[42] are indicated on the ordinates. Concentrations of the matrices are indicated at the far right in each case. All three tracers show that the self-diffusion limit ($M = M_p$), indicated by an arrow in each case, is substantially different from the asymptotic tracer diffusion coefficient D_{tr}^∞ at $M \ll M_p$. These data sets show that when M_p is at least 3–5 times larger than M, the asymptotic diffusion coefficients D_{tr}^∞ can be obtained.

D_{tr}^∞, at sufficiently high matrix molecular weight that the matrix molecular weight dependence vanishes. We call attention to our experimental conditions first; the matrix molecular weight is so chosen that its concentration is at least 3 times the overlap concentration in order to ensure the semidilute condition. From now on, we call the asymptotic tracer diffusion coefficients D_{tr}^∞ just the diffusion coefficients, and they are collected in Table II and plotted as a function of matrix concentration in Figure 4. Similar to the case of self-diffusion shown in Figure 1, D_{tr}^∞ drops sharply as the concentration of the matrix increases. The self-diffusion data of 900k labeled polystyrene shown in Figure 1 are reproduced as a dashed curve in the same plot for comparison. Note that the diffusion coefficients are about a factor of 2–3 smaller than those of self-diffusion over the semidilute range. As noted in the previous section, this point appeared to have escaped experimental scrutiny in the literature.

The diffusion coefficients at zero matrix concentration represent the values obtained by extrapolation to the infinite dilution limit, and they are seen to match very well with the mutual diffusion coefficients measured by QELS as well as with other literature values.[42] At this limit, the polymer chains diffuse with fully developed hydrodynamic interactions inside the chain and the hydrodynamic radius has a molecular weight dependence similar to that of the radius of gyration of the whole chain. As the matrix concentration increases, the hydrodynamic screening length ξ, i.e., the size of the concentration blobs formed by interpenetration of matrix chains, decreases; it eventually reaches the size of diffusant at a matrix concentration equal to the overlap concentration of the tracer

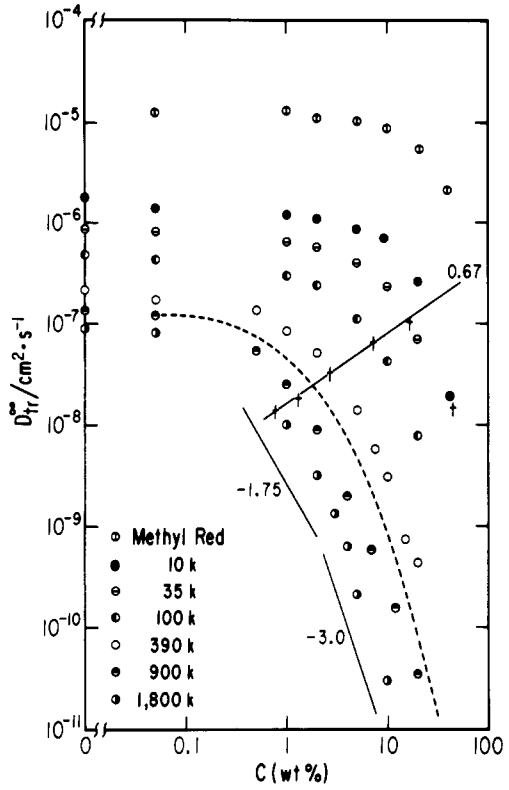

Figure 4. Matrix concentration dependence of D_{tr}^{∞} at 20 °C in toluene. Different symbols refer to the tracer polymer molecular weights M except for methyl red. The tracer concentration in each series is 0.05 wt %. In all cases, the data at 0.05 wt % (without matrix polymer) are the self-diffusion coefficients, which compare favorably with D_0 values in the literature, which are indicated on the ordinate. In all cases, the matrix molecular weights M_p were large enough that the tracer diffusion coefficients reached their asymptotic values, D_{tr}^{∞}. For comparison, the self-diffusion coefficients of 900k polystyrene (Figure 1) are overlaid as a dashed curve. D_{tr}^{∞} at C^* of a given tracer is estimated[43] by an empirical relationship and it is marked with a dagger for each tracer series. Such $D_{tr}^{\infty}(C^*)$ give rise to a slope of 0.67 as shown, except for the 10k sample (see text). Though all data sets can best be represented by smooth curves, −1.75 and −3.0 slopes (scaling predictions in a good solvent in the semidilute regime and at the Θ-condition, respectively) are drawn for comparison.

polymer. The diffusion coefficients at such points are estimated by interpolation of D_{tr}^{∞} to C^* using the empirical relation[43] $C^* = 620M^{-0.785}$, and these are marked by daggers in Figure 4. According to the scaling argument, these diffusion coefficients should follow the same concentration dependence as that of the mutual diffusion coefficient in the semidilute regime. The prediction is confirmed here; we can draw a straight line with the same slope, 0.67, as that of the mutual diffusion coefficient through the points even though the two sets of diffusion coefficients differ by a few orders of magnitude. The deviation from the straight line at high concentration is an expected behavior since the local friction should be much different from that at low concentration. In other words, it is no longer a semidilute solution by definition. We should use this deviation for the purpose of local friction correction, rather than the change of small-molecule tracer diffusion coefficients as was proposed earlier by Nemoto et al.,[32] since the tracer diffusion coefficients of "blobs" include the necessary hydrodynamic interactions. As can be seen, the local friction does not seem to play a significant role up to the concentration of 15 wt %, beyond which it begins to exhibit a pronounced effect. Therefore, we can conclude that it is safe to treat the data up to 15 wt % without accounting for the change of local friction. From these observations,

Table II
Asymptotic Tracer Diffusion Coefficient Polystyrene in Various Matrices

tracer	matrix	C/(wt %)	D_{tr}^{∞}/(cm^2/s)
1800k		0	8.1 (±0.4) × 10^{-8}
	8400k	1	1.0 (±0.1) × 10^{-8}
	8400k	2	3.2 (±0.3) × 10^{-9}
	8400k	3	1.34 (±0.09) × 10^{-9}
	8400k	4	6.4 (±0.4) × 10^{-10}
	8400k	5	2.08 (±0.18) × 10^{-10}
	8400k	10	3.01 (±0.13) × 10^{-11}
900k		0	1.2 (±0.2) × 10^{-7}
	8400k	0.5	5.4 (±0.3) × 10^{-8}
	8400k	1	2.5 (±0.3) × 10^{-8}
	8400k	2	9.0 (±0.6) × 10^{-9}
	8400k	4	2.0 (±0.1) × 10^{-9}
	8400k	7	6.9 (±0.6) × 10^{-10}
	8400k	12	1.57 (±0.16) × 10^{-10}
	8400k	20	3.5 (±0.4) × 10^{-11}
390k		0	1.7 (±0.2) × 10^{-7}
	8400k	0.5	1.35 (±0.10) × 10^{-7}
	8400k	1	8.5 (±0.4) × 10^{-8}
	8400k	2	5.0 (±0.3) × 10^{-8}
	8400k	5	1.3 (±0.1) × 10^{-8}
	1800k	7	5.7 (±0.3) × 10^{-9}
	1800k	10	3.2 (±0.2) × 10^{-9}
	1800k	15	7.3 (±1.0) × 10^{-10}
	1800k	20	4.39 (±0.06) × 10^{-10}
100k		0	4.3 (±0.3) × 10^{-7}
	3800k	1	3.0 (±0.2) × 10^{-7}
	1800k	2	2.5 (±0.1) × 10^{-7}
	600k	5	1.1 (±0.1) × 10^{-7}
	600k	10	4.2 (±0.3) × 10^{-8}
	600k	20	7.7 (±0.5) × 10^{-9}
35k		0	8.2 (±0.3) × 10^{-7}
	3800k	1	6.4 (±0.3) × 10^{-7}
	1800k	2	5.9 (±0.4) × 10^{-7}
	600k	5	4.0 (±0.1) × 10^{-7}
	390k	10	2.3 (±0.1) × 10^{-7}
	100k	20	7.0 (±0.1) × 10^{-8}
10k		0	1.38 (±0.06) × 10^{-6}
	3800k	1	1.20 (±0.04) × 10^{-6}
	1800k	2	1.08 (±0.06) × 10^{-6}
	600k	5	8.8 (±0.2) × 10^{-7}
	390k	9.3	7.0 (±0.7) × 10^{-7}
	100k	20	2.6 (±0.2) × 10^{-7}
	100k	42.1	1.93 (±0.08) × 10^{-8}
methyl red		0	1.26 (±0.09) × 10^{-5}
	900k	1	1.35 (±0.08) × 10^{-5}
	900k	2	1.14 (±0.08) × 10^{-5}
	900k	5	1.03 (±0.05) × 10^{-5}
	900k	10	8.8 (±0.6) × 10^{-6}
	51k	2	1.11 (±0.08) × 10^{-5}
	51k	5	1.07 (±0.06) × 10^{-5}
	51k	10	8.6 (±0.5) × 10^{-6}
	51k	21	5.8 (±0.9) × 10^{-6}
	51k	40	2.10 (±0.07) × 10^{-6}

we can say that the hydrodynamic screening in a semidilute solution and its concentration dependence are confirmed.

Another interesting observation near the overlap concentration is shown in Figure 5. The decay profile of the FRS signal in the vicinity of C^* markedly deviates from a single-exponential decay as seen in dilute solution. This probably reflects local inhomogeneity of the scale of ξ in the polymer matrix. Therefore, the diffusant feels a nonuniform environment, particularly when its size is similar to the screening length of the system. In other words, the tracer polymer chains are sieved most actively near the overlap concentration. A puzzling issue however is how any inhomogeneity in the scale of ξ (10^2–10^3 Å) could be manifested in the length scale of fringe spacing,

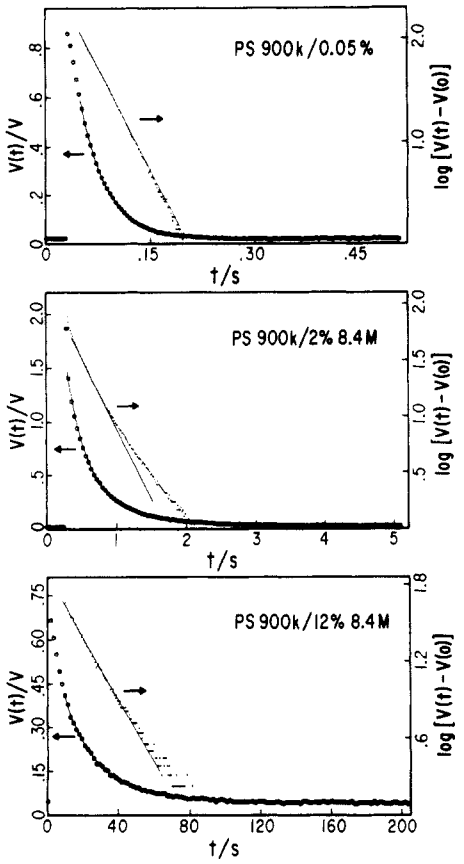

Figure 5. FRS signal profiles of 900k tracer sample by itself and in two different concentrations of 8400k matrix. The tracer polymer by itself at 0.05 wt % (top) shows a clean single-exponential profile for two logarithmic decades in time. In the middle profile, a substantial departure from single exponential is seen for 2 wt %, corresponding to $C \approx C^*$ of the tracer polymer. In the bottom profile, the FRS signal appears to recover partially the single exponentiality at a matrix concentration of 12%. Similar trends were seen for all cases and particular departures from single exponentiality were observed at a matrix concentration close to C^* as marked by daggers in Figure 4. This may be explained by a sieving effect of the tracers by the finite mesh size (or screening length) distribution $G(\xi)$ of the matrix polymer. Also, this effect can be seen most prominently when the size of a tracer is close to the average screening length $\langle \xi \rangle$.

d = 3–20 μm. Though our efforts were somewhat cursory, we could not detect any dependence on the fringe spacing relative to the departure from single-exponential decay. On the other hand, we can clearly rule out the sample heterogeneity as the cause since recovery from the departure is observed where it should have been most pronounced in the higher concentration region; i.e., $D \propto M^{-3}$. It is evident that this observation must be pursued in further detail in order to come to grips with the intriguing puzzle.

Molecular Weight Dependence of D_{tr}^{∞}. In Figure 6 is shown the diffusant molecular weight dependence of D_{tr}^{∞}. With no matrix polymer present we clearly observe power law behavior with a slope −0.6. Since our tracer polymer concentration is only 0.05 wt %, this dilute solution behavior showing the Flory exponent in a good solvent is to be expected. As matrix concentration increases, D_{tr}^{∞} depends more sensitively on M beyond −0.6. These are easily recognized by smooth curves drawn over the experimental data. The arrow on each curve designates the molecular weight of the diffusant beyond which the semidilute regime should prevail at the given concentration. From all profiles it is easily discerned that there exists no well-defined unique exponent over a wide molecular weight range, and the dependence is greater as M gets larger. We note here that error bars on individual datum points are slightly larger than the drawn circles on the log–log scale of the figure, so they are not shown explicitly; however, the numerical values of the errors are collected in Table II. Hence, even with error bars included in the plot, we can cleanly claim that the observed M dependence is progressively varying; in fact, if we insist on an exponent, we can find a limited molecular weight range showing −2.0 exponent just above c^*, but the slope quickly becomes steeper than −2.0. In particular, the data for 10 and 20 wt % show a substantial range of M where the dependence is clearly better represented by −3.0 exponent.

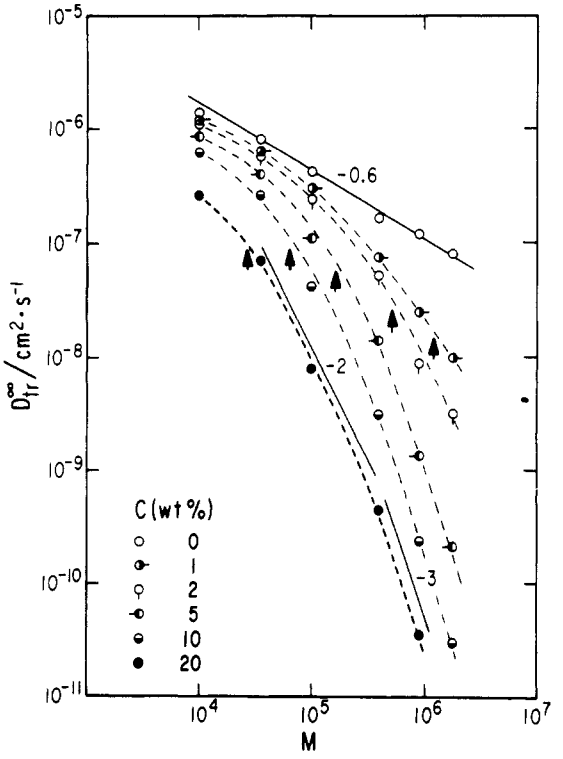

Figure 6. Plot of D_{tr}^{∞} vs. tracer molecular weight M at different matrix concentrations. Error bars of individual datum points are slightly larger than the circles; hence they are not shown (however, the numbers are collected in Table II). The matrix concentrations are distinguished by different symbols. In all cases, the tracer concentration is 0.05 wt %, and at this concentration the tracers by themselves exhibit infinite dilution behavior in a good solvent, $D_0 \propto M^{-0.6}$, and this is shown by the straight line at the top. As the concentration is increased the M dependence becomes progressively more sensitive, and at 20 wt % the apparent power law exponent ranges from −1 to −3.

Not having the data beyond M = 1800k, it is difficult to extrapolate how the dependence should vary from −3.0 exponent. In any event, the most likely applicable exponent is greater than −2.0, which is the reptation prediction in the high-molecular-weight and high-concentration regimes. Given that we are dealing with tracer diffusion in the limit of large molecular weight of the matrix, the reptation condition should best be fulfilled by these matrices. We further note that the −2 exponent has been observed by many in bulk as well as in semidilute solutions. To the best of our knowledge, this departure from the −2 exponent is the first such observation. In order to examine this behavior further, we turn to Figure 7a, where $M^2 D_{tr}^{\infty}$ is plotted as a function of matrix concentration. At first glance, M^2 scaling makes a universal curve above C^*, and a reasonable power law region with −1.75 slope is found at a relatively low concentration range but still above C^*.

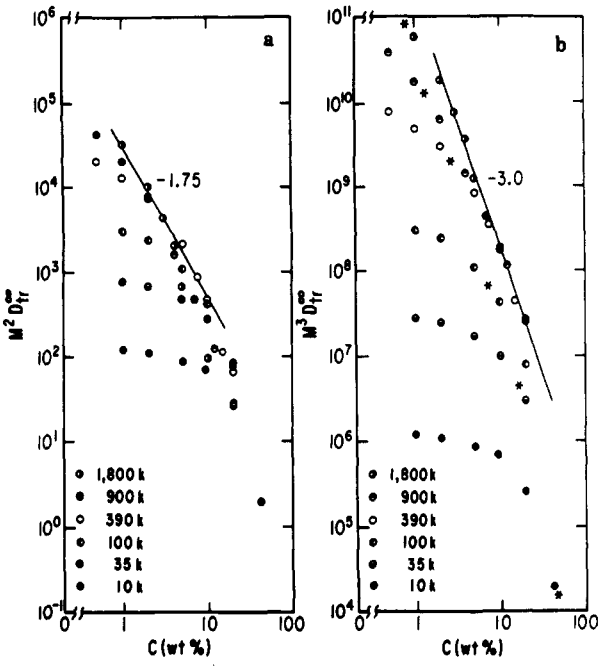

Figure 7. (a) Double-logarithmic plot of $M^2D_{tr}^{\infty}$ vs. C. All data are plotted to show where the concentration dependence of D_{tr}^{∞} follows a power law of −1.75. (b) Double-logarithmic plot of $M^3D_{tr}^{\infty}$ vs. C; an asterisk in each series designates C^* of the tracer.

At higher concentrations and for higher diffusant molecular weights, however, such a scaling fails to yield a universal curve. When we apply the correction for local friction using the "blob friction coefficient" discussed in the previous section, they get closer to the power law line but not enough to put all the points on a universal curve. If we examine Figures 6 and 7 carefully, those points deviating from a concentration power law also deviate from a molecular weight power law behavior, and vice versa. Obviously something is missing to take account of both concentration and molecular weight dependences of the diffusion coefficients.

Alternatively, we can try with $M^3D_{tr}^{\infty}$ against C. This is shown in Figure 7b. The concentration power law of −3 appears to give a better universality, except for a few points just above overlap concentration. In order to clarify the semidilute range in each molecular weight series, an asterisk is marked for C^* on each series. The results make it apparent that we can recast $D_{tr}^{\infty} \propto M^{-2}C^{-1.75}$ into $D_{tr}^{\infty} \propto M^{-3}C^{-3}$ with the same set of data. We thus come to the inescapable conclusion that our data are not uniquely explained by the reptation prediction.

At this point one may argue that ours is the only anomaly to bring about a discordance with the reptation model, which seems to "account for" most of the previous diffusion experiments. We, of course, can hardly cast doubt on the validity of the reptation model based solely on this set of data. Instead, we are mostly concerned with whether the reptation prediction has been frequently used with due consideration given to the basic criterion for its application. It can be shown that one can predict the power law dependence of C if the corresponding one of M is given and vice versa using a simple scaling argument. It depends on a scaling behavior of $D_{tr}^{\infty}(C)$ with (C/C^*) if $C > C^*$:

$$D_{tr}^{\infty}(C) = D_{tr}^{\infty}(C^*)(C/C^*)^x \tag{4}$$

and

$$C^* = M/R_g^3 \tag{5}$$

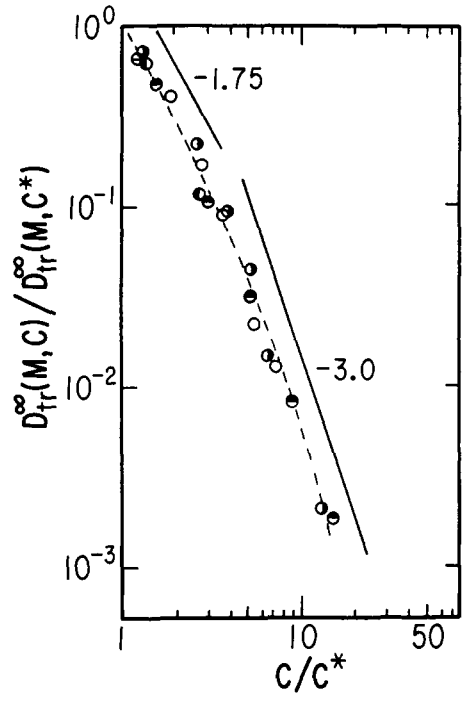

Figure 8. Double-logarithmic plot of $D_{tr}^{\infty}(C)/D_{tr}^{\infty}(C^*)$ vs. (C/C^*). The values of $D_{tr}^{\infty}(C^*)$ are the interpolated ones given in Figure 4 as (†), and C^* is calculated from the empirical relation $C^* \approx 620M^{-0.785}$.[43] Error bars of individual datum points are slightly larger than the circles. The dashed curve is the best fit to a trial function, eq 6, with $a = 1.77$ and $b = 23.4$.

If we assume that $D_{tr}^{\infty}(C)$ is proportional to M^{-m}, and $D_{tr}^{\infty}(C^*)$ to $M^{-\nu}$, then x turns out to be $(\nu - m)/(3\nu - 1)$. Thus, we can have the set $\{m, x\}$ as (1, −0.25), (2, −1.75), and (3, −3) for three simple cases when $\nu = 0.6$ for a good solvent. An empirical test of eq 4 is exhibited in Figure 8, where $D_{tr}^{\infty}(C)/D_{tr}^{\infty}(C^*)$ is plotted as a function of (C/C^*) on a log–log scale. We see that all the data points of different M merge to form a universal curve, and our scaling analysis according to eq 4 seems to work reasonably well for the range of $35\,000 \leq M \leq 1\,800\,000$. Note here also that error bars on individual datum points are only slightly larger than drawn circles, so we have chosen not to show them. In order to test whether the suggested concentration scalings are indeed borne out by the data, we fit the entire set to the following trial function:

$$\log \{D_{tr}^{\infty}(C)/D_{tr}^{\infty}(C^*)\} = \{-a - [(C/C^*)/b]\} \log (C/C^*) \tag{6}$$

where a and b are the adjustable fitting parameters. The result of such a fit is shown in the figure as the dashed curve and the parameters are found as $a = 1.77 \pm 0.08$ and $b = 23.4 \pm 4.6$. Thus, the test appears quite positive, at least relative to −1.75 slope, whereas −3 slope in the vicinity of $C/C^* \approx 5$ could easily be replaced by progressively changing slope. Of course, there is no theoretical basis for eq 6, whereas $x = -3$ has a scaling basis if $m = 3$, and this is shown to be the case in Figure 7. In any event, the plot confirms the universal behavior of $D_{tr}^{\infty}(C)/D_{tr}^{\infty}(C^*)$ relative to (C/C^*) invariant of M and that is the point of eq 4. Further, our interpolated data in Figure 4, marked, with daggers, confirm one of the above assumptions, $D_{tr}^{\infty}(C^*) \propto M^{-\nu}$. If we assume at this point that the observed molecular weight dependence is not derived from the reptation theory, then the concentration power exponent has no bearing on the assumed diffusion mechanism. In other words, a different concentration dependence can be easily expected in the region where a different molecular weight

dependence is observed. For example, we can get the $C^{-3.0}$ dependence shown in Figure 7b in the high-concentration range by using the $M^{-3.0}$ dependence observed at the same concentration region in Figure 6. This makes our argument self-consistent. Of course, we have no basis to justify how $M^{-3.0}$ should arise; hence we cannot offer any plausible alternative to the reptation process. What we claim here is that the reptation prediction is not uniquely confirmed by our experiments, and the same could be said of other experimental results. Perhaps the current rush to confirm the reptation model by experiment should be tempered by a more critical evaluation of the results.

Conclusions

We can summarize our results as follows.

1. In semidilute solutions, there is a substantial matrix molecular weight dependence of the tracer diffusion coefficient. Also, it was found that matrix molecular weight dependence vanishes only when it reaches at least a factor of 3–5 higher than that of the diffusant.

2. In the framework of the reptation model, the proposed tube renewal process does not appear to be weak in the semidilute regime.

3. The hydrodynamic screening concepts in semidilute solutions are proven to be valid by this tracer diffusion measurement. We could reproduce the same concentration dependence of the screening length, $\xi \propto C^{0.67}$, as that found in other dynamic measurements such as quasi-elastic light scattering.

4. The local friction change does not appear to be significant up to the concentration of 15 wt %, and the simple scaling argument for semidilute solution should be valid below this concentration even if local friction change is not taken into account.

5. The tracer diffusion coefficients deviate from the prediction of the reptation model for high molecular weight diffusants at high concentrations of matrix. This raises the question of whether the reptation model can correctly represent the diffusion process of polymer chains in semidilute solutions.

6. An alternative scaling argument was used to interpret our data. There appears to exist a reasonable scaling relation between $D_{tr}^{\infty}(C)/D_{tr}^{\infty}(C^*)$ and (C/C^*) and we can adopt a different molecular weight dependence than the reptation model to account for the observed concentration dependence and vice versa.

Acknowledgment. This work was in part supported by the National Science Foundation (Polymers Program) and Kodak Research Laboratories. We also acknowledge the donors of the Petroleum Research Fund, administered by the American Chemical Society, for partial support of this research. It is a pleasure to thank Dr. Elizabeth V. Patton of Kodak Research Laboratories for a thorough characterization of one of the samples. Also, valuable discussions with Drs. K. L. Ngai and G. B. McKenna are gratefully acknowledged.

Registry No. $C_6H_5CH_3$, 108-88-3; polystyrene, 9003-53-6.

References and Notes

(1) de Gennes, P.-G. *Scaling Concepts in Polymer Physics*; Cornell University: Ithaca, NY, 1979.
(2) de Gennes, P.-G. *J. Chem. Phys.* **1971**, *55*, 572.
(3) de Gennes, P.-G. *Macromolecules* **1976**, *9*, 587, 594.
(4) Doi, M.; Edwards, S. F. *J. Chem. Soc., Faraday Trans. 2* **1978**, *74*, 1789, 1802, 1818.
(5) Bueche, F. *J. Chem. Phys.* **1968**, *48*, 1410.
(6) Klein, J. *Nature (London)* **1978**, *271*, 143. Klein, J.; Briscoe, B. J. *Proc. R. Soc. London, Ser. A* **1979**, *365*, 53.
(7) Bartel, C. R.; Graessley, W. W.; Crist, B. *J. Polym. Sci., Polym. Lett. Ed.* **1983**, *21*, 495; *Macromolecules* **1984**, *17*, 2702.
(8) Stejskal, E. O.; Tanner, J. E. *J. Chem. Phys.* **1965**, *42*, 288. Tanner, J. E. *Macromolecules* **1971**, *4*, 748.
(9) Léger, L.; Hervet, H.; Rondelez, F. *Macromolecules* **1981**, *14*, 1732.
(10) Wesson, J. A.; Noh, I.; Kitano, T.; Yu, H. *Macromolecules* **1984**, *17*, 782.
(11) Antonietti, M.; Coutandin, J.; Grütter, R.; Sillescu, H. *Macromolecules* **1984**, *17*, 798.
(12) Smith, B. A. *Macromolecules* **1982**, *15*, 469.
(13) Green, P. F.; Mills, P. J.; Palmstrøm, C. J.; Mayer, J. W.; Kramer, E. J. *Phys. Rev. Lett.* **1984**, *53*, 2145.
(14) Green, P. F.; Palmstrøm, C. J.; Mayer, J. W.; Kramer, E. J. *Macromolecules* **1985**, *18*, 501.
(15) Tirrell, M. *Rubber Chem. Technol.* **1984**, *57*, 523.
(16) von Meerwall, E.; Grigsby, J.; Tomich, D.; Van Antwerp, R. *J. Polym. Sci., Polym. Phys. Ed.* **1982**, *20*, 1037.
(17) Klein, J. *Macromolecules* **1978**, *11*, 852.
(18) Daoud, M.; de Gennes, P.-G. *J. Polym. Sci., Polym. Phys. Ed.* **1979**, *17*, 1971.
(19) Klein, J.; Fletcher, D.; Fetters, L. J. *Faraday Symp. Chem. Soc.* **1983**, *18*, 159.
(20) McKenna, G. B.; Hadziioannou, G.; Lutz, P.; Hild, G.; Strazielle, C.; Rempp, P.; Kovacs, A. J. *Bull. Am. Phys. Soc.* **1984**, *29*, 408.
(21) Roovers, J. *Macromolecules* **1985**, *18*, 1359; Mills, P. J.; Mayer, J. W.; Kramer, E. J.; Hadziioannou, G.; Lutz, P.; Strazielle, C.; Rempp, P.; Kovacs, A. J. *Bull. Am. Phys. Soc.* **1985**, *30*, 490.
(22) Doi, M. *Polym. Prepr. (Am. Chem. Soc., Div. Polym. Chem.)* **1981**, *22*(1), 100.
(23) Klein, J. *Polym. Prepr. (Am. Chem. Soc., Div. Polym. Chem.)* **1981**, *22*(1), 105.
(24) Graessley, W. W. *Adv. Polym. Sci.* **1982**, *47*, 67.
(25) Graessley, W. W. *J. Polym. Sci., Polym. Phys. Ed.* **1980**, *18*, 27.
(26) Lin, Y. H. *Macromolecules* **1984**, *17*, 2846.
(27) Fujita, H.; Einaga, Y. *Polym. J. (Tokyo)* **1985**, *17*, 1131.
(28) McKenna, G. B.; Ngai, K. L.; Plazek, D. J. *Polymer* **1985**, *26*, 1651.
(29) Deutch, J. M. *Phys. Rev. Lett.* **1985**, *54*, 56.
(30) Callaghan, P. T.; Pinder, D. N. *Macromolecules* **1984**, *17*, 431.
(31) Fleischer, G.; Straube, E. *Polymer* **1985**, *26*, 241.
(32) Nemoto, N.; Landry, M. R.; Noh, I.; Kitano, T.; Wesson, J. A.; Yu, H. *Macromolecules* **1985**, *18*, 308.
(33) Adam, M.; Delsanti, M. *Macromolecules* **1977**, *10*, 1229.
(34) Roots, J.; Nyström, B.; Sundelöf, L. O.; Porsh, B. *Polymer* **1979**, *20*, 337.
(35) Mitchell, A. R.; Kent, S. B. H.; Erickson, B. W.; Merrifield, R. B. *Tetrahedron Lett.* **1976**, *42*, 3795.
(36) Sheehan, J. C.; Hess, G. P. *J. Am. Chem. Soc.* **1955**, *77*, 1067.
(37) Sheehan, J. C.; Goodman, M.; Hess, G. P. *J. Am. Chem. Soc.* **1956**, *78*, 1367.
(38) Wesson, J. A.; Takezoe, H.; Yu, H.; Chen, S. P. *J. Appl. Phys.* **1982**, *53*, 6513.
(39) Salcedo, J. R.; Siegman, A. E.; Dlott, D. D.; Fayer, M. D. *Phys. Rev. Lett.* **1978**, *41*, 131.
(40) Munch, J. P.; Candau, S.; Herz, J.; Hild, G. J. *J. Phys. (Paris)* **1977**, *38*, 971.
(41) Nyström, B.; Roots, J. *J. Macromol. Sci., Rev. Macromol. Chem.* **1980**, *C19*, 35.
(42) Appelt, B.; Meyerhoff, G. *Macromolecules* **1980**, *13*, 657.
(43) Adam, M.; Delsanti, M. *J. Phys. (Paris)* **1983**, *44*, 1185.